NASA TECHNICAL MEMORANDUM 89135

CONVERGENCE OF STRAIN ENERGY RELEASE RATE COMPONENTS FOR EDGE-DELAMINATED COMPOSITE LAMINATES

I. S. Raju, J. H. Crews, Jr., and M. A. Aminpour

APRIL 1987

National Aeronautics and Space Administration

Langley Research Center
Hampton, Virginia 23665

CONVERGENCE OF STRAIN ENERGY RELEASE RATE COMPONENTS FOR EDGE-DELAMINATED COMPOSITE LAMINATES

I. S. Raju*, J. H. Crews, Jr+., and M. A. Aminpour&
NASA Langley Research Center
Hampton, Va 23665-5225

ABSTRACT

Strain energy release rates for edge-delaminated composite laminates were obtained using quasi three-dimensional finite element analysis. The problem of edge-delamination at the -35/90 interfaces of an eight ply $[0/\pm35/90]_s$ composite laminate subjected to uniform axial strain was studied. A quasi three-dimensional finite element analysis was used to calculate the total and individual components of the strain energy release rate. The individual components did not show convergence as the delamination tip elements were made smaller. In contrast, the total strain energy release rate, G, converged and remained unchanged as the delamination tip elements were made smaller and agreed with the total G calculated using a closed-form equation derived from the rule of mixtures and classical laminated plate theory. The studies of the near-field solutions for a delamination at an interface between two dissimilar isotropic or orthotropic plates showed that the imaginary part of the singularity is the cause of the nonconvergent behavior of the individual components. To evaluate the

* Senior Scientist, Analytical Services and Materials, Inc., Hampton, Va.
+ Senior Scientist, Materials Division
& Research Scientist, Analytical Services and Materials, Inc., Hampton, Va.
(Work performed under NASA Contract NAS1-18256.)

accuracy of the results, an eight ply $[0/\pm35/r/90]_s$ laminate with the delamination modeled in a thin resin layer, similar to the resin layer that exists between the -35 and 90 plies, was analyzed. Because the delamination exists in a homogeneous isotropic material, the oscillatory component of the singularity vanishes. The strain energy release rates remained unchanged as the delamination tip elements were made smaller. Comparison of the strain energy release rates for the 'bare' interface laminate, i.e. one without the resin layer, and for the laminate with the resin showed that the 'bare' interface models are a very good approximation for the resin case if the delamination tip elements were one-quarter to one-half of the ply thickness.

INTRODUCTION

Composites are used extensively in aerospace, automobile, and civil engineering structures because of their high strength-to-weight ratios. Because delamination is a common failure mechanism of composite laminates, research has been directed toward understanding delamination mechanisms and quantifying the strength of composite laminates with delaminations [1,2].

Recently, to quantify the interlaminar fracture toughness of composite laminates, the edge-delamination test was proposed in references 1-3. For the family of $[0/\pm\theta/90]_s$ laminates subjected to remote uniform axial strain, O'Brien [2] found that for a given interlaminar fracture toughness the minimum failure strain was obtained when $\theta = 35^o$. Therefore, the $[0/\pm35/90]_s$ family of laminates, consisting of $[\pm35/0/90]_s$, $[35/0/-35/90]_s$, and $[0/\pm35/90]_s$ layups, was recommended for the edge-

delamination test. In this family of laminates, the interlaminar normal stresses are greatest when the delamination is between the 90^{o} ply and its neighbor. For these laminates, the total strain-energy release rate for self-similar delamination growth can be obtained using an equation derived from the rule of mixtures and the classical laminated plate theory (CLT) [1]. However, the individual components (mode I, mode II, and mode III) cannot be determined from simple formulas like that given in reference 1. To determine the individual components, the boundary value problem of the laminate with edge-delaminations needs to be solved. The quasi-three dimensional (Q3D) finite element analyses are useful to determine the interlaminar stresses and the strain energy release rates for delamination growth.

The laminates used in the edge-delamination test are cocured. Experimental evidence indicates that very thin resin-rich layers of about 0.0004 in. thick exist between neighboring plies [5,6]. The Q3D finite element analysis should model these resin layers as well as the individual plies. Because the resin layers are very thin and smooth transitions are needed in the model, large numbers of elements and nodes are required to model the resin layers. Therefore, the resin layers are usually neglected and the delamination is assumed to be at a discrete interface between neighboring plies [1-4,7]. In reference 3, a $[0/\pm35/90]_{s}$ laminate with a 'bare' interface was modeled with 8-noded isoparametric parabolic elements everywhere. At the delamination tip, square non-singular parabolic elements were used. The convergence of the strain energy release rates was studied for various size delamination tip elements. The study showed that the

individual components of the strain energy release rates did not converge as the size of the delamination tip elements was reduced. Therefore, the accuracy of the individual components determined by such a model is questionable. In contrast, the total strain energy release rate converged to show no change with the reduction of the size of delamination tip elements. Also the total strain energy release rate agreed extremely well with that calculated using the CLT formula from reference 1.

The first objective of this paper is to identify the source of the non-convergent behavior of the individual components of strain energy release rate. The second objective is to establish the accuracy of the finite element solution for the 'bare' interface problem. To this end, a cocured laminate with resin-rich interfaces was analyzed and compared to a 'bare' interface model.

First, the edge-delamination problem and the Q3D finite element analyses are reviewed. Then the strain energy release rates for the $[0/\pm35/90]_s$ laminate with a 'bare' interface between -35 and 90 plies were obtained using either non-singular or quarter-point singularity elements at the delamination tip. The singularity elements were used to determine if the use of the non-singular elements was the cause for the non-convergent behavior of the individual components. While the quarter-point elements produce the classical square root singularity at the delamination tip, the singularity at the delamination tip between two dissimilar materials is known to be of the form $-1/2 \pm i\gamma$ for two-dimensional (2D) problems [7-11]. The imaginary part of the singularity, the so called "oscillatory"

component, γ, may also be a cause for the non-convergence of the individual components. To study this aspect, the near field stress distribution for cracks between dissimilar isotropic or orthotropic materials under plane stress or plane strain was examined. Next, the edge-delamination problem with delamination between two different isotropic materials was studied using the Q3D finite element analysis with the oscillatory component either zero or non zero. Last, the strain energy release rates for a $[0/\pm35/90]_s$ laminate obtained with a resin interface are presented for various size delamination tip elements. These results are compared with those obtained without modeling the resin layer.

SYMBOLS

a	length of delamination
b	half width of the laminate
E_{jj}	Young's modulus for orthotropic material in the j-direction
E_r	Young's modulus of resin
G	total strain energy release rate
G_I, G_{II}, G_{III}	mode I, mode II, and mode III strain energy release rate components, respectively
G_{jk}	shear modulus for orthotropic material
h	ply thickness
h_r	resin thickness
i	$\sqrt{-1}$
t	total thickness of the laminate
U,V,W	displacement functions

u,v,w	displacements in the x-, y-, and z-directions, respectively
x,y,z	Cartesian coordinates
Δ	delamination tip element size
ϵ_o	uniform axial strain in the x-direction
$\{\epsilon\}$	Cartesian engineering strains, $\{ \epsilon_x, \epsilon_y, \epsilon_z, \epsilon_{xy}, \epsilon_{yz}, \epsilon_{zx} \}$
μ_j	shear modulus for the j^{th} isotropic material
$\{\sigma\}$	Cartesian stresses, $\{ \sigma_x, \sigma_y, \sigma_z, \sigma_{xy}, \sigma_{yz}, \sigma_{zx} \}$
γ	oscillatory part of the singularity
ν_j	Poisson's ratio of the j^{th} isotropic material
ν_{jk}	Poisson's ratio for orthotropic material
ν_r	Poisson's ratio of the resin
θ	angle between x-axis and the fiber axis (see fig 1(a))

Superscript

bar denotes complex conjugate

EDGE-DELAMINATION ANALYSIS

A symmetric eight ply laminate subjected to uniform axial strain ϵ_o in the x-direction is shown in Fig. 1. Delaminations at both edges are located symmetrically about the laminate midplane (at the -35/90 interface above the midplane and at the 90/-35 interface below the midplane). Because the laminate is long in the x-direction, all x=constant planes away from the ends deform in the same manner. Therefore, away from the ends the displacements are assumed to be,

$$u = U(y,z) + \epsilon_o x$$
$$v = V(y,z) \qquad (1)$$
$$w = W(y,z)$$

where U,V,W are displacement functions expressed in terms of y and z alone [4,7,12,13]. Equations (1) describe a 'quasi three-dimensional' (Q3D) problem. The modifier 'quasi' is used because there are three displacements in the three directions, but the gradients of U, V, and W with respect to the x-coordinate are zero. Thus only an x=constant plane needs to be analyzed to obtain the stresses in the laminate. Figure 1(b) shows a typical x=constant plane. Because of symmetries, only one quarter of this plane was analyzed (see Figure 2).

The material properties used in this study were

$$E_{11} = 19.5 \times 10^6 \text{ psi} \; ; \; E_{22} = E_{33} = 1.48 \times 10^6 \text{ psi}$$
$$\nu_{12} = \nu_{13} = 0.3 \; ; \; \nu_{23} = .49$$
$$G_{12} = G_{13} = 0.8 \times 10^6 \text{ psi} \; ; \; G_{23} = 0.497 \times 10^6 \text{ psi}$$

where the subscripts 1, 2, and 3 correspond to the longitudinal, transverse, and thickness directions of a zero degree ply [3,7]. The resin properties used in this study are $E_r = .5 \times 10^6$ psi ; $\nu_r = .3$. These properties gives a shear modulus of 0.192×10^6 psi.

When subjected to axial strain, the 0/±35 ply group above the delamination tends to contract (and shear) by different amounts in the y-direction (and the xy-plane) compared to the 90 ply below the delamination. Therefore,to maintain the displacement continuity along the -35/90 interface (z=h in Figure 2), σ_y and σ_{xy} stresses develop in the interior as shown in figure 2. Equilibrium requires that stresses σ_{yz}, σ_{xz}, and σ_z exist along

the z = h interface (see fig 2(b)). Because the faces of the delamination are stress free, these interlaminar stresses exist only in the range $0 \leq y \leq (b-a)$. These interlaminar stress give rise to three modes of deformation at the delamination tip.

Figure 3(a) shows modeling for the edge-delamination in Fig 1(b). Two types of modeling were used. In the first model, 8-noded isoparametric parabolic elements were used to model the region. In this model, these non-singular elements were used everywhere including the delamination tip. The second model was identical to the first, except collapsed quarter-point singularity elements were used around at the delamination tip, as shown in Fig. 3(b). The details of the Q3D analysis are given in reference 4 and hence, are not repeated here.

The total strain energy release rate, G, was obtained from CLT as,

$$G = \frac{\epsilon^2_o t}{2n} [E_{LAM} - E^*] \qquad (2)$$

where E_{LAM} and E^* are axial stiffnesses calculated from the classical laminated plate theory (CLT) for the undelaminated and completely delaminated laminates (along one or more interfaces), respectively [1,2]. The n is the number of delaminated interfaces, and t is the total laminate thickness. As previously mentioned, the individual components of strain energy release rate cannot be obtained by simple formulas like equation 2. However, these components can be calculated using a Q3D finite element analysis [1-4,7].

The components of strain energy release rate were calculated using forces and displacements near the delamination tip with Irwin's virtual crack closure technique (VCCT) as,

$$G_I = - \frac{1}{2\Delta} [F_{zi} \{ t_{11} (W_m - W_m') + t_{12} (W_k - W_k') \} + F_{zj} \{ t_{21} (W_m - W_m') + t_{22} (W_k - W_k') \}] \quad (3)$$

where F_{zi} is the force in the z-direction at node i, W_m is the W-displacement at node m, etc. (see Fig. 4) [14,15]. For non-singular elements (see Fig 4(a)), $t_{11} = 1$; $t_{12} = 0$; $t_{21} = 0$; $t_{22} = 1$ and for quarter-point singularity elements (see Fig 4(b)), $t_{11} = 6-(3\pi/2)$; $t_{12} = 6\pi-20$; $t_{21} = 1/2$; $t_{22} = 1$. Similar expressions for G_{II} and G_{III} were used with F_z replaced by F_y and F_x and with W replaced by V and U, respectively.

Several finite element idealizations were used with both the non-singular and singular elements. Delamination tip element sizes were Δ/h = 0.5, 0.25, 0.125, and 0.0625. In the finite element analysis with non-singular elements, the singularity at the delamination tip is not modeled. On the other hand, when the quarter-point elements are used the square root singularity is incorporated at the delamination tip. The VCCT was used with both element types to evaluate the strain energy release rates. Table 1 presents the individual and the total strain energy release rates calculated with non-singular and quarter-point singularity elements, respectively. These results are also plotted in Fig 5. Both the non-singular and the singular elements yielded similar results. They showed that the total strain energy release rate remained unchanged as the size of the delamination tip elements decreases. However, both element type shows a

slight non-convergence for the individual modes. This situation is in contradiction to the conventional belief that better accuracy may be obtained when the size of the crack/delamination tip elements are decreased. The mode-I strain energy release rate becomes larger as the delamination tip element becomes smaller (i.e. for smaller values of Δ/h). The mode-II strain energy release rate shows the opposite trend. The mode-III component has a very small negative value. The total strain energy release rate computed from the finite element analysis agrees very well with that calculated by equation (2).

ANALYSIS OF NON-CONVERGENCE

In this section, the reasons for the non-convergence of the individual components of the strain energy release rate are explored. In the edge-delamination problem the delamination exists at the interface between two different anisotropic materials. For this case the singularity is not the classical square root singularity but is of the form $r^{-1/2\pm i\gamma}$, where r is the radial distance measured from the delamination tip. The γ depends on the material properties of the two materials [7-11]. This imaginary power leads to the stress oscillations very close to the delamination tip. The oscillatory component of the singularity may cause the non-convergence of the individual G components. To explore this possibility, a simpler problem of a bi-material plate in plane stress or plane strain was studied.

The problem of an interfacial crack in a bi-material plate with two different isotropic materials in either plane stress or plane strain was

examined. Then, the same problem with two orthotropic materials was studied.

Interfacial Crack in Bi-Material Isotropic Plate

Figure 6 shows a bi-material plate with an interfacial crack subjected to remote uniform tension. Due to the applied stress, each of the two materials tries to contract differently. Because they are joined at the interface (z=0), to maintain continuity a shear stress σ_{yz} develops along the bond line. Thus a mixed mode condition develops for remote tension. However, for certain combinations of material properties that satisfy Eq. A5 (see appendix) , the contractions very close to the crack tip are identical and hence the shear stresses σ_{yz} are not required to maintain the continuity. On the other hand, if two materials do not satisfy Eq. A5, then shear stress stresses σ_{yz} are needed on the z=0 line to maintain compatibility and the near field stress state will be different from the classical square root distribution and is of the form,

$$\sigma_z = (Pr^{-1/2 +i\gamma} + \bar{P}r^{-1/2 -i\gamma}) + \ldots$$
$$\sigma_{yz} = (Rr^{-1/2 +i\gamma} + \bar{R}r^{-1/2 -i\gamma}) + \ldots \qquad (4)$$

where P and R are complex constants, and $\bar{P}$ and $\bar{R}$ are their corresponding complex conjugates [8-11]. These constants depend on the loading. The oscillatory power, γ ,in Eq. (4) is given by,

$$\gamma = \frac{1}{2\pi} \ln \left[\frac{\mu_A + \mu_B k_A}{\mu_B + \mu_A k_B} \right] \qquad (5)$$

where μ_j are the shear moduli and k_j are given by

$$k_j = 3 - 4\nu_j \quad \text{for plane strain and}$$

$$= \frac{3 - \nu_j}{1 + \nu_j} \quad \text{for plane stress}$$

and j= A,B.

When the two materials satisfy Eq. A5 the oscillatory power, γ, is identically zero because the terms in the square brackets in Eq. 5 become unity.

From the results in reference 11, it can be shown that the constants P and R in Eq. 4 are related to each other as $R = -iP$. The relative displacements of the crack faces behind the crack tip have the form

$$\begin{aligned} v &= (Sr^{1/2+i\gamma} + \bar{S}r^{-1/2-i\gamma}) + \ldots \\ w &= (Qr^{1/2+i\gamma} + \bar{Q}r^{-1/2-i\gamma}) + \ldots \end{aligned} \qquad (6)$$

where the constants Q and S are complex constants and are related to each other as $S = -iQ$.

The strain energy release rates for the crack along the interface of this bi-material plate can be determined as outlined below.

Strain Energy Release Rates

The strain energy release rates were obtained by using the near field solution of Eqs. 4 and 6 and Irwin's VCCT as,

$$G = \lim_{\Delta \to 0} \frac{1}{2\Delta} \int_0^{\Delta} [\ \sigma_z(r).w(\Delta - r) + \sigma_{yz}(r).v(\Delta - r)\ ]\ dr \qquad (7)$$

where Δ is now the distance over which the crack is assumed to close. (Note that in the finite element analysis Δ was the delamination tip element size.)

The mode I and mode II components of the strain energy release rates are

$$G_I = \lim_{\Delta \to 0} \frac{1}{2\Delta} \int_0^{\Delta} [\ \sigma_z(r).w(\Delta - r)\ ]\ dr$$

$$G_{II} = \lim_{\Delta \to 0} \frac{1}{2\Delta} \int_0^{\Delta} [\ \sigma_{yz}(r).v(\Delta - r)\ ]\ dr \qquad (8)$$

Substituting the stresses and displacements from Eqs 4 and 6 into Eqs. (8) gives,

$$G_I = \lim_{\Delta \to 0} [\ PQ\Delta^{2i\gamma}\ I_1 + \bar{P}\bar{Q}\Delta^{-2i\gamma}\ \bar{I}_1 + \bar{P}Q\ I_2 + P\bar{Q}\ \bar{I}_2\ ] \qquad (9)$$

where

$$I_1 = \int_0^{\pi/2} \cos^2\beta\ (\sin\beta\ \cos\beta)^{2i\gamma}\ d\beta$$

$$I2 = \int_0^{\pi/2} \cos^2\beta\ (\cos\beta/\sin\beta)^{2i\gamma}\ d\beta \qquad (10)$$

$$= (\pi/2)\ (2i\gamma + 1)/(\ e^{\pi\gamma} + e^{-\pi\gamma}\ )$$

The integral I_1 in Eq. (10) is the Beta function. The integrals in Eq. (10) can be evaluated for known values of γ .

G_{II} was obtained similarly as,

$$G_{II} = \lim_{\Delta \to 0} [\ RS\Delta^{2i\gamma}\ I_1 + \overline{RS}\Delta^{-2i\gamma}\ \overline{I}_1 + \overline{R}S\ I_2 + R\overline{S}\ \overline{I}_2\ ] \qquad (11)$$

Because $R = -iP$ and $S = -iQ$, equation 11 reduces to

$$G_{II} = \lim_{\Delta \to 0} [\ -PQ\Delta^{2i\gamma}\ I_1 - \overline{PQ}\Delta^{-2i\gamma}\ \overline{I}_1 + \overline{P}Q\ I_2 + P\overline{Q}\ \overline{I}_2\ ] \qquad (12)$$

Equations (9) and (12) show that the mode I and mode II strain energy release rates depend on Δ . The terms $\Delta^{\pm 2i\gamma}$ can be rewritten as $e^{\pm 2i\gamma \ln(\Delta)}$. As Δ approaches zero, the exponential functions have no well defined limits; they oscillate between +1 and -1. In the finite element analysis, this means that the computed mode I and mode II strain energy release rates will be dependent on the crack tip element size and do not show convergence as the crack tip elements are made smaller.

The total strain energy release rate is the sum of G_I and G_{II} (see Eq. 7) and is

$$\begin{aligned} G &= G_I + G_{II} \\ &= \lim_{\Delta \to 0} [\ 2\overline{P}Q\ I_2 + 2P\overline{Q}\ \overline{I}_2\ ] \\ &= [\ 2\overline{P}Q\ I_2 + 2P\overline{Q}\ \overline{I}_2\ ] \end{aligned} \qquad (13)$$

The terms involving $\Delta^{\pm 2i\gamma}$ do not appear in the total strain energy release rate. The total strain energy release rate is therefore independent of Δ. This analysis suggests that the total strain energy release rate will converge as the crack tip element size decreases but the individual mode components depend on Δ, and hence, do not converge.

On the other hand, if the two materials are so chosen that the oscillatory power, γ , is equal to zero (i.e when $\mu_A + \mu_B k_A = \mu_B + \mu_A k_A$), the mode I and mode II components in Eq. (9) and (12) do not depend on Δ and, thus, have a finite limit. Thus when $\gamma=0$, the individual as well as the total strain energy release rates must converge as the size of the crack tip elements decreases.

Interfacial Crack in a Bi-material Orthotropic Plate

Instead of the two isotropic plates considered earlier, consider a crack between two orthotropic materials. The singularity at the crack tip is also of the form $-1/2 \pm i\gamma$ [7,11]. The near field stress and displacement distributions have a similar form as Eqs. 4 and 6, but the expressions for P,Q,R, and S are too complex to write symbolically due to the complex functional forms. Therefore, the plane strain problem of two orthotropic materials subjected to remote tension was analyzed with a special crack tip singularity element which utilizes the near field solution that contains the oscillatory component at the crack tip [11]. From the numerical solution the constants P,Q,R, and S were evaluated for different combinations of orthotropic materials. The constants satisfied the following relations for all combinations:

$$PQ + RS = 0 \text{ and } \overline{P}Q = \overline{R}S \qquad (14)$$

This means that like the isotropic case, for the bi-material orthotropic case the total strain energy release rates are independent of Δ (see Eqs (9) and (12)). Again, the individual components G_I and G_{II} will dependent on Δ,

because of the $\Delta^{\pm 2i\gamma}$ term in equations like 9 and 12. Thus the finite element solutions for the bi-material orthotropic case show trends like the bi-material isotropic case.

The previous discussion is centered on plane problems. However, the focus problem is a Q3D problem. The Q3D problem can be thought of as a superposition of two problems. Problem 1 is with $\epsilon_x = \epsilon_o$ and the rest of the five strains are zero. Problem 2 is with $\epsilon_x = 0$ and the rest of the strains are non zero (see Eq. (1)). Problem 1 yields the non-homogeneous part of the solution, while problem 2 yields the homogeneous part. Thus one can concentrate on problem 2 to understand the behavior of the solution. But problem 2 is exactly equivalent to the plane strain problem. Thus the previously presented analysis for the plane problems is also valid for the Q3D problem under consideration.

RESULTS AND DISCUSSION

To evaluate the analysis presented in the previous section, an edge-delamination problem was studied using a laminate with two isotropic materials having zero or non-zero values of γ. Next, the edge-delamination problem was analyzed using a resin-rich layer at the interface. The strain energy release rates for the resin layer case were compared with those from a 'bare' interface model to evaluate the accuracy of the 'bare' interface model.

Laminate with Isotropic Materials

To demonstrate that the oscillatory part of the singularity is the cause of the non-convergence of the individual mode components, a laminate consisting of two isotropic materials A and B with ply thicknesses 3h and h, respectively, and a delamination at z = h was considered (i.e in Fig. 2(a), the top three plies are of material A and the bottom ply is of material B). Materials A and B had the following properties:

Material A : $E_A = 10 \times 10^6$ psi ; $\nu_A = 0.3$

Material B : $E_B = 19.231 \times 10^6$ psi ; $\nu_B = 0.0$

These materials were chosen so that the $\gamma = 0$ for plane strain conditions. Table 2 presents the individual as well as the total strain energy release rates when various size non-singular and quarter-point elements were used at the delamination tip. The finite element solutions yielded almost identical results for various element sizes at the delamination tip.

Next, the material properties of the ply below the delamination was changed to

Material B : $E_B = 30 \times 10^6$ psi ; $\nu_B = 0.0$

From equation (5), this combination of materials gives a non-zero oscillatory power 0.087. Table 3 presents the strain energy release rates for this material combination with non-singular and quarter-point elements at the delamination tip. As expected, the individual modes do not convergence as the delamination tip elements are made smaller but the total strain energy release rate remains practically unchanged with mesh refinement. These results confirm that the oscillatory part of the

singularity is the cause of the non-convergence of the individual mode components.

Laminates with Orthotropic materials

As pointed out earlier, the stress singularity for delamination between two orthotropic materials is also of the form $-1/2 \pm i\gamma$ [7,11]. For the particular material properties considered and for the $[0/\pm35/90]_s$ laminate with a delamination at the -35/90 interface, the singularity is $-0.5 \pm 0.0225i$ [7,16]. (This value is determined by interpolation of values given in reference 7). The isotropic results presented earlier, indicates that the oscillatory part of the singularity is causing the non-convergence of the individual modes presented in Table 1.

As pointed out in the introduction, in reality, a discrete or 'bare' interface does not exist between plies as was assumed earlier. When the laminates are cured, a thin resin layer develops between the neighboring plies. This resin layer is about 0.0004 in. thick. For convenience, the delamination was assumed to exist centrally within this resin layer. An eight ply laminate, $[0/\pm35/r/90]_s$, with a delamination in the interface resin layer was analyzed. Note that the resin layer at interfaces other than the delaminated interface were not modeled because their influence on the strain energy release rates was considered negligibly small owing to their small thicknesses. As the delamination exists in a homogeneous isotropic material (the interface resin layer), the singularity has the classical square root power without the oscillatory component. Thus, the

individual components of the total strain energy release rate should converge as the size of the delamination tip elements are decreased.

Three finite element idealizations with Δ/h_r = 0.25, 0.125, and 0.0625 were developed, where h_r is the resin thickness (h_r/h = 0.074). At the delamination tip, square non-singular elements were used. The finite element models had about 1800 nodes and about 5400 degrees of freedom. This large number of nodes was required because smooth transition was needed away from the delamination tip, and the delamination tip elements in the resin layer were much smaller than those used in the 'bare' interface models. Table 4 presents results obtained with these models. As expected, the individual as well as the total strain energy release rates showed very little change the for various values of Δ/h_r values. Also, the G_{III} component is now positive.

The 'bare' interface laminate was reanalyzed with the same physical delamination tip elements as the resin layer model. Table 5 presents the results with this model. Note that the model here has delamination tip elements that are an order of magnitude smaller than those presented in Table 1. These results show the same nonconvergent behavior as Table 1 results. The results for the resin layer model (Table 4) and the 'bare' interface results of Tables 1 and 5 are plotted in Fig. 7. Note that Δ/h on the abscissa is plotted on the log scale. The horizontal dashed line represents the mode I and mode II components for the laminate with a thin resin layer at the delaminated interface. The results for the laminate with the 'bare' interface are not vastly different from those with the cocured

laminate if Δ/h values between 0.25 and 0.5 are used. However, larger discrepancies exist if much smaller Δ/h values are used. The maximum differences are less than 4 percent for mode I and about 2 percent for mode II if Δ/h values of 0.25 or 0.5 are used. Therefore, the finite element model with the 'bare' interface (Δ/h = 0.25 or 0.5) was a very good approximation to the case with the interface resin layer, although this model suffers from the non-convergence of the individual modes as the delamination tip elements are made smaller. This model is attractive because fewer elements are required and, hence, fewer degrees of freedom. The present results suggest that the size of the delamination tip elements should be one-quarter to one-half of the ply thickness.

CONCLUSIONS

The problem of edge-delamination of a long $[0/\pm35/90]_s$ composite laminate subjected to uniform axial strain was studied. This laminate had edge-delaminations at the -35/90 interfaces. Finite element models had either a ' bare' interface or a thin resin layer at the interface. A quasi three-dimensional finite element analysis was used to calculate the strain energy release rates. The virtual crack closure technique was used to obtain the individual components as well as the total strain energy release rates.

The finite element analysis showed that the individual components of strain energy release rate did not converge when the ratio of the size of the delamination tip element to the ply thickness, (Δ/h), decreased for the 'bare' interface case. In contrast, the total strain energy release rates

were unchanged as Δ/h decreased and agreed very well with the value calculated from a closed form equation derived from the rule of mixtures using classical laminated plate theory. This non-convergence was observed with non-singular, 8-noded parabolic elements and with collapsed quarter-point singularity elements at the delamination tip. However, the results obtained using the non-singular and singular elements agreed very well with each other.

Results for the resin layer case showed that the individual components as well as the total strain energy release rates remain practically unchanged as Δ/h decreased. Based on the studies performed, the following conclusions are drawn:

1. The non-convergence of the individual components of the strain energy release rate calculated by quasi three-dimensional finite element analyses is due to the oscillatory part of the stress singularity. Continuum analyses show that the individual components will have no definite limit as the virtual crack closure size approaches zero. The total strain energy release rate, in contrast, has a well defined limit.

2. When the materials were chosen such that the oscillatory component of the singularity is zero, the finite element solutions showed convergence for the individual components as well as for the total strain energy release rates as Δ/h was decreased This is in agreement with the continuum analyses.

3. When values of Δ/h were either 0.25 or 0.5, the individual components of the strain energy release rate obtained with the 'bare' interface model agreed well with those obtained with the resin layer model. The maximum difference between the two models was less than 4 percent for the mode I and 2 percent for the mode II components.

APPENDIX

RELATIONSHIP BETWEEN THE MATERIAL PROPERTIES FOR EQUAL CONTRACTIONS ϵ_y NEAR THE CRACK TIP

The purpose of this appendix is obtain a relationship between the material properties of materials A and B such that the contractions in the y-direction very near the crack tip are identical (see Fig. 6). Consider the stresses σ_z and σ_y in the two materials very near the crack tip and along the z = 0 line,

$$\sigma_{zA} = \sigma_{zB} = \frac{K_I}{\sqrt{2\pi r}} \qquad \sigma_{yA} = \sigma_{yB} = \frac{K_I}{\sqrt{2\pi r}} \tag{A1}$$

The corresponding strains are

$$\epsilon_{yA} = [\sigma_{yA} - \nu_A \sigma_{zA} - \nu_A \sigma_{xA}]/E_A \tag{A2}$$

and

$$\epsilon_{yB} = [\sigma_{yB} - \nu_B \sigma_{zB} - \nu_B \sigma_{xB}]/E_B \tag{A3}$$

where

$$\sigma_{xj} = 0 \quad \text{for plane stress}$$
$$= \nu_j (\sigma_{yj} + \sigma_{zj}) \quad \text{for plane strain,} \tag{A4}$$

and j=A,B.

If the strains ϵ_y are same for the two materials A and B then by equating Eq. (A2) and (A3) one can show that

$$\mu_A + \mu_B k_A = \mu_B + \mu_A k_B \tag{A5}$$

The μ_A and μ_B are the shear moduli of materials A and B, respectively, and k_j is given by,

$$k_j = \begin{cases} 3 - 4\,\nu_j & \text{for plane strain and} \\ \dfrac{3 - \nu_j}{1 + \nu_j} & \text{for plane stress} \end{cases} \qquad \text{(A6)}$$

and j= A,B.

Thus if the material properties of the two materials are such that Eq. (A5) is satisfied then the stress-distribution very near the crack tip is given by Eq. (A1) and it does not contain the oscillatory part γ . However, if the material properties do not satisfy Eq. (A5) then the simple square root distribution alone cannot maintain the compatibility along the bond line and very near the crack tip.

REFERENCES

1. T. K. O'Brien," Characterization of delamination onset and growth in a composite laminate", in Damage in Composite Materials, ASTM STP 775, 1982, pp. 140-167.

2. T. K. O'Brien," Mixed-mode strain energy release rate effects on edge-delamination ", in Effects of Defects in Composite Materials, ASTM STP 836, 1984, pp. 125-142.

3. T. K. O'Brien, N. J. Johnston, I. S. Raju, D. H. Morris, and R. A. Simmonds," Comparisons of various configurations of the edge-delamination test for interlaminar fracture toughness", in Toughened Composites, ASTM STP 937, 1987. (Also available as NASA TM-86433, July 1985.)

4. I. S. Raju, "Q3DG- A Computer program for strain-energy release rates for delamination growth in composite laminates", NASA CR-178205, November 1986.

5. H. Chai, "Bond thickness in adhesive joints and its significance for mode I interlaminar fracture of composites", in Composite Materials: Testing and Design (Seventh Conference), ASTM STP 893, 1986, pp. 209-231.

6. J. H. Crews, Jr., K. N. Shivakumar and I. S. Raju, "Factors influencing elastic stresses in double cantilever beam specimens", NASA TM-89033, November 1986.

7. S. S. Wang and I. Choi, "The mechanics of delamination in fibre-reinforced composite laminates. Part I- Stress singularities and solution structure. Part II- Delamination behavior and fracture mechanics parameters", NASA CR 172269 and 172270, November 1983.

8. M. L. Williams," The stresses around a fault or crack in dissimilar media", Bulletin of Seismology Society of America, Vol. 49, 1959, pp. 199-204.

9. B. M. Malyshev and R. L. Salganik, "The strength of adhesive joints using the theory of fracture", Int. J. Fracture Mech. Vol 1, 1965, pp. 114-128.

10. F. Erdogan and G. D. Gupta, " Layered composites with an interface flaw", Int. J. of Solids and Structures, Vol. 7, 1971, pp. 1089-1107.

11. M. A. Aminpour, " Finite element analysis of propagating interface cracks in composites ", Ph. D. Dissertation, University of Washington, March 1986. (Also available from University Microfilms, Ann Arbor, Michigan).

12. A. S. D. Wang and F. W. Crossman," Some new results on edge effects in symmetric composite laminates", J. of Composite Materials, Vol. 11, 1977, pp. 92-106.

13. I. S. Raju and J. H. Crews, Jr.," Interlaminar stress singularities at a straight free edge in composite laminates", J. of Computers and Structures, Vol. 14, 1981, pp. 21-28.

14. E. F. Rybicki and M. F. Kanninen," A finite element calculation of stress intensity factors by modified crack closure integral", Engineering Fracture Mechanics, Vol. 9, 1977, pp. 931-938.

15. I. S. Raju," Simple formulas for strain energy release rates with higher order and singular finite elements", NASA CR 178186, September 1986.

16. S. S. Wang," Edge-delamination in angle-ply composite laminates", AIAA Jnl., Vol. 22, No. 2, 1984, pp 256-264.

Table 1: Individual and total strain energy release rates for a $[0/\pm35/90]_s$ laminate : Non-singular and quarter-point singularity elements.

	Percentage of individual modes			
Δ/h =	0.5	0.25	0.125	0.0625
Mode I	21.22	22.41 (21.89)*	23.49 (23.38)	24.65 (24.69)
Mode II	79.98	78.82 (79.10)	77.76 (77.61)	76.58 (76.31)
Mode III	-1.20	-1.23 (-0.99)	-1.25 (-0.99)	-1.24 (-1.00)
$\frac{G}{\epsilon^2_o \, t \, E_{11}}$	0.0407	0.0406 (0.0402)	0.0407 (0.0402)	0.0406 (0.0401)

* Values in parentheses obtained with quarter-point singularity elements.

$[\, G/(\epsilon^2_o \, t \, E_{11})]_{CLT} = 0.0407$

Table 2: Individual and total strain energy release rates for a laminate with two isotropic materials: Non-singular and quarter-point singularity elements.

$E_A = 10x\ 10^6$ psi ; $\nu_A = 0.3$

$E_B = 19.231x\ 10^6$ psi ; $\nu_B = 0.0$

$\gamma = 0.0$

	Percentage of individual modes		
Δ/h =	0.25	0.125	0.0625
Mode I	39.20 (38.76)*	39.21 (38.82)	39.19 (38.78)
Mode II	60.80 (61.24)	60.70 (61.18)	60.81 (61.22)
Mode III	0.0	0.0	0.0
$\frac{G}{\epsilon^2_o\ t\ E_A}$	0.0137 (0.0137)	0.0137 (0.0137)	0.0137 (0.0137)

* Values in parentheses obtained with quarter-point singularity elements.

$[\ G/(\epsilon^2_o\ t\ E_A)]_{CLT} = 0.0137$

Table 3: Individual and total strain energy release rates for a laminate with two isotropic materials: Non-singular and quarter-point singularity elements.

$E_A = 10 \times 10^6$ psi ; $\nu_A = 0.3$

$E_B = 30 \times 10^6$ psi ; $\nu_B = 0.0$

$\gamma = 0.087$

	Percentage of individual modes for		
Δ/h =	0.25	0.125	0.0625
Mode I	47.81 (46.94)*	49.44 (48.59)	51.06 (50.19)
Mode II	52.19 (53.06)*	50.56 (51.41)	49.94 (49.81)
Mode III	0.0	0.0	0.0
$\frac{G}{\epsilon^2_o \, t \, E_A}$	0.0177 (0.0178)	0.0177 (0.0177)	0.0177 (0.0177)

* Values in parentheses obtained with quarter-point singularity elements.

$[\, G/(\epsilon^2_o \, t \, E_A)]_{CLT} = 0.0177$

Table 4: Individual and total strain energy release rates for a $[0/\pm35/r/90]_s$ laminate with delamination in the resin layer: Non-singular elements.
($h = 0.0054$ in.; $h_r = 0.0004$ in.; $h_r/h = 0.074$)

	Percentage of individual modes		
Δ/h_r =	0.25	0.125	0.0625
Mode I	18.65	18.68	18.68
Mode II	81.13	81.10	81.09
Mode III	0.22	0.22	0.23
$\frac{G}{\epsilon^2_o \, t \, E_A}$	0.0404	0.0404	0.0404

$[\, G/\, (\epsilon^2_o \, t \, E_A \,)]_{CLT} = 0.0404$; Here $t = 8h$.

Table 5: Individual and total strain energy release rates for a $[0/\pm35/90]_s$ laminate with delamination between -35 and 90 plies: Non-singular elements.

	Percentage of individual modes		
Δ/h =	0.0370	0.0185	0.00925
Mode I	25.53	26.74	28.00
Mode II	75.68	74.43	73.12
Mode III	-1.21	-1.17	-1.12
$\frac{G}{\epsilon^2_o \, t \, E_{11}}$	0.0406	0.0406	0.0406

$[\, G/\, (\epsilon^2_o \, t \, E_{11}\,)]_{CLT} = 0.0407$

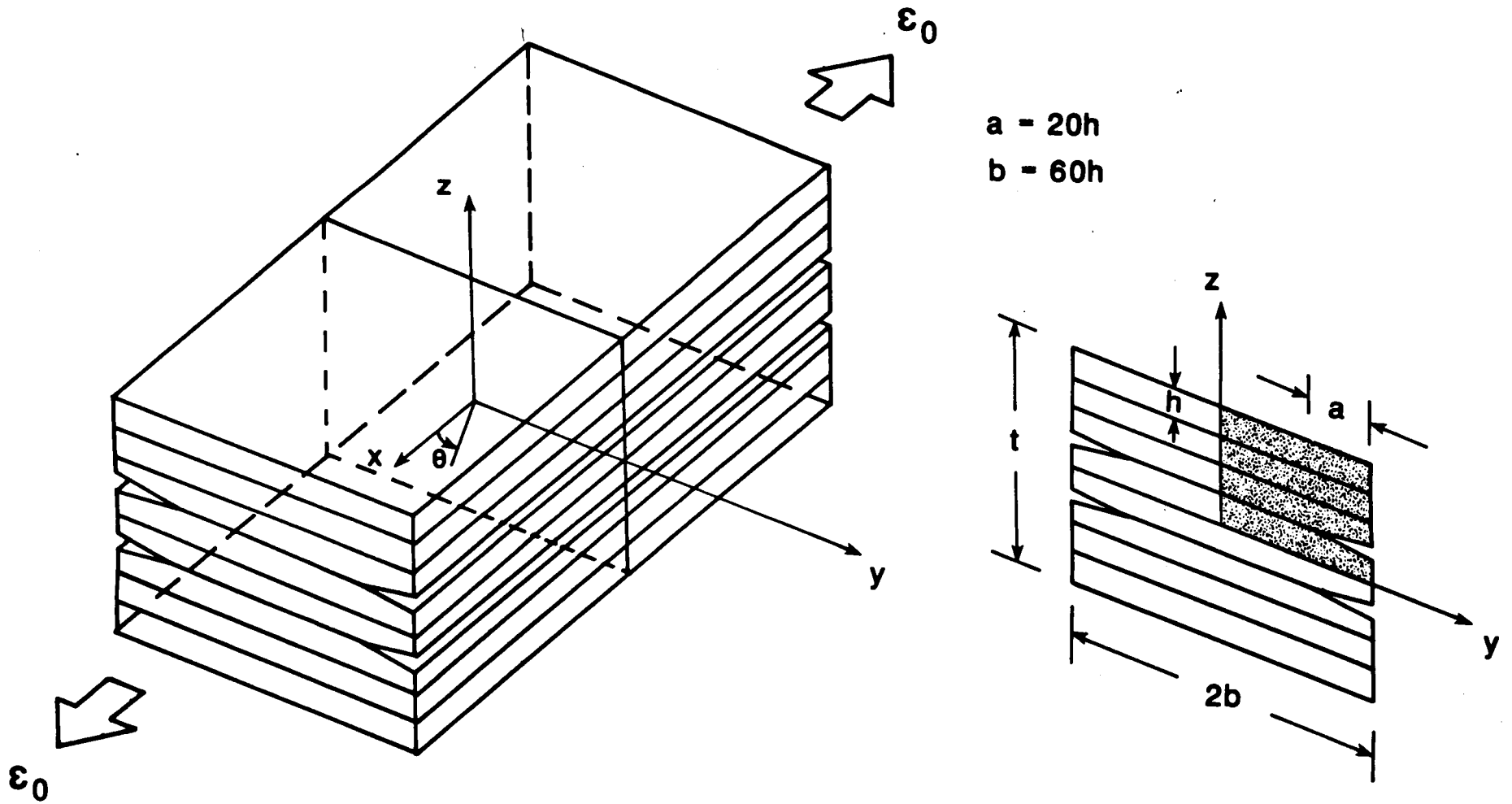

(a) Delaminated eight ply laminate

(b) Typical x = constant plane

Fig. 1: Laminate configuration and analysis region

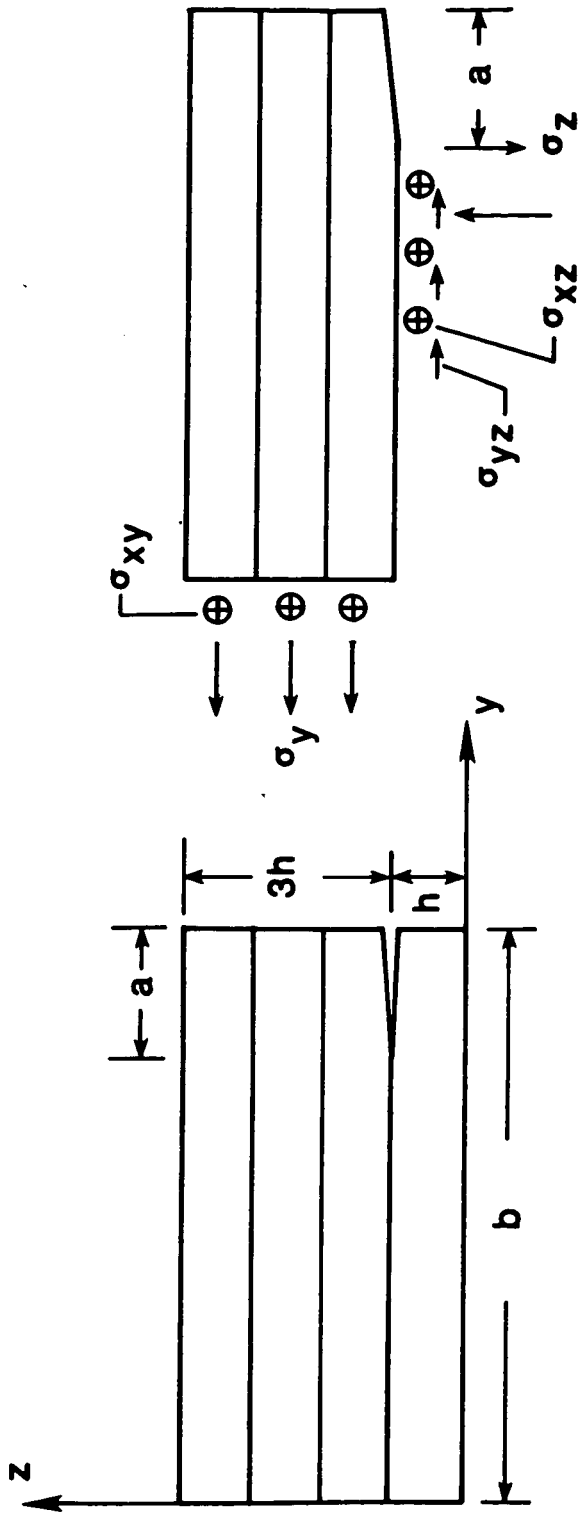

Fig.2: Typical x=constant plane and free body diagram showing equilibrium of top group of plies

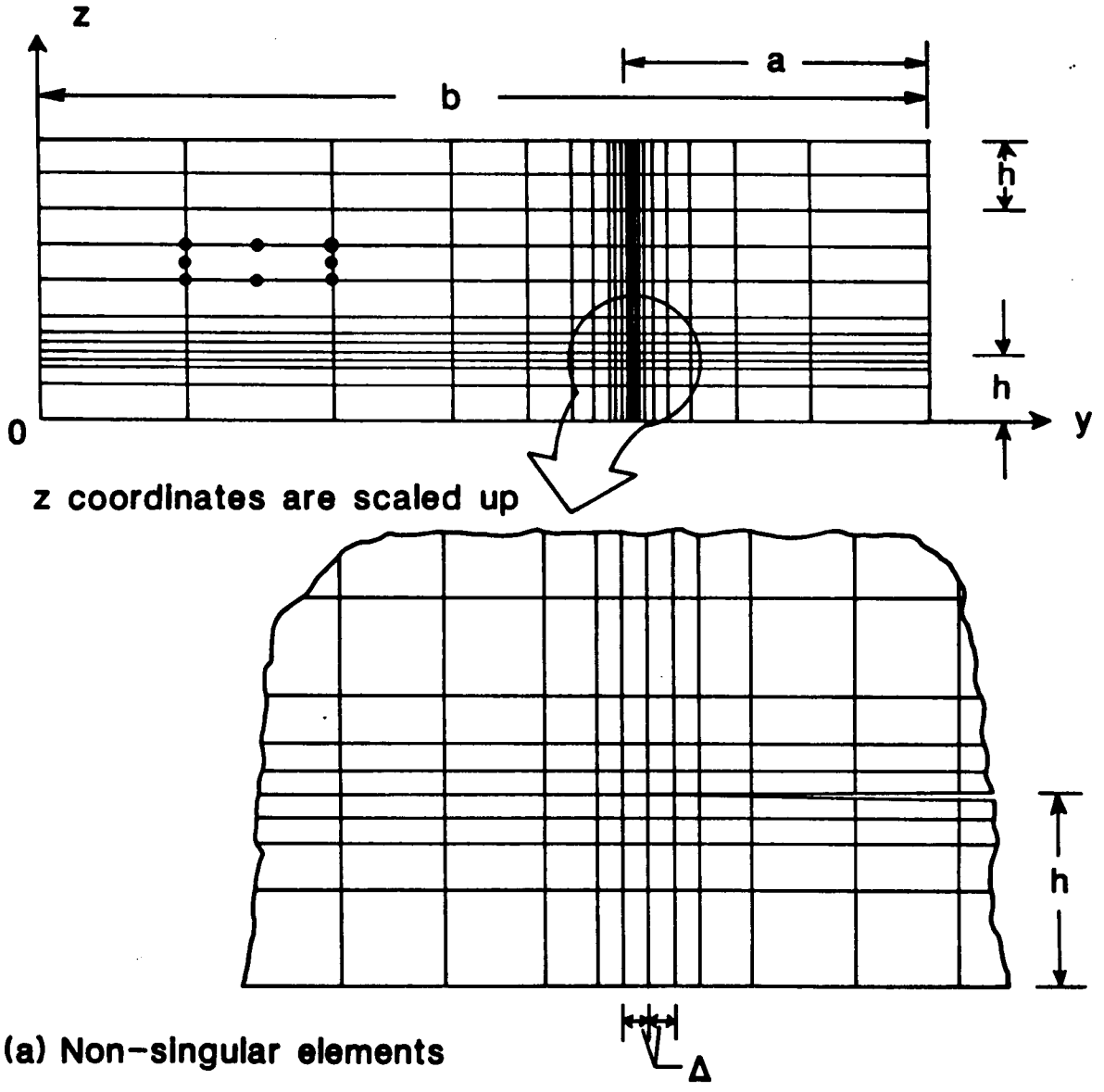

(a) Non-singular elements

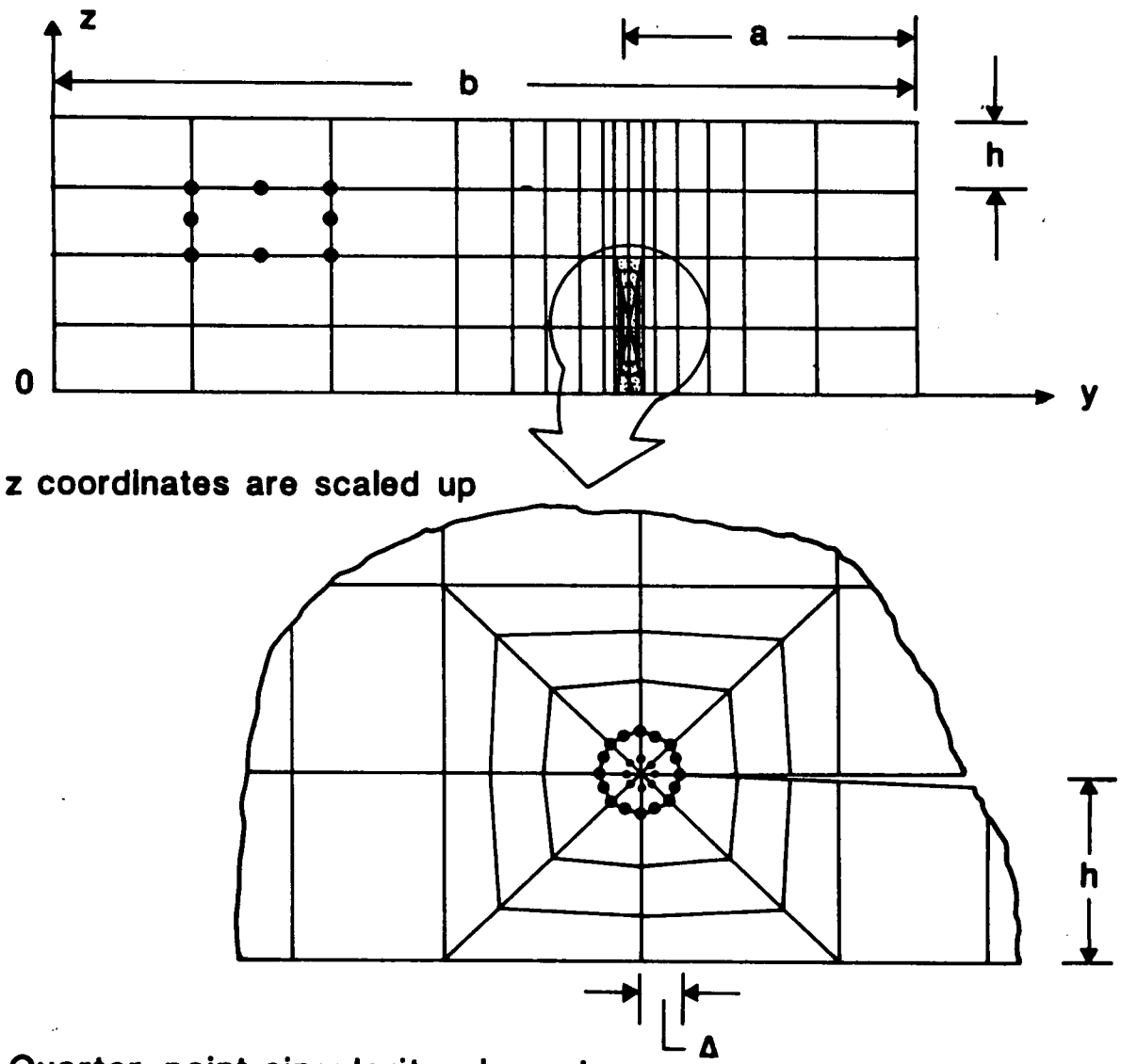

(b) Quarter-point singularity elements

Fig.3: Finite element models

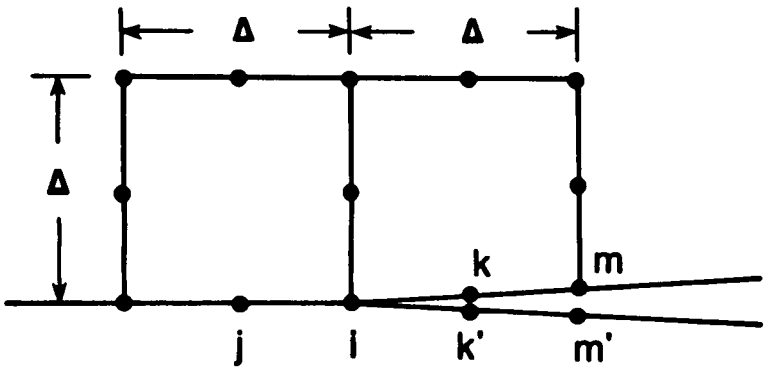

(a) Non-singular elements

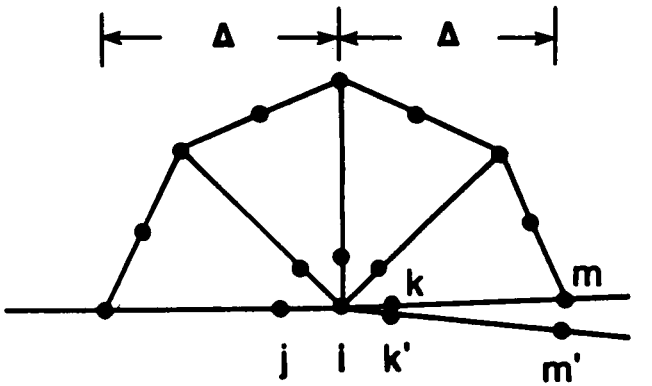

(b) Collapsed quarter-point singularity elements

Fig.4: Nodes used in the strain energy release rate calculations

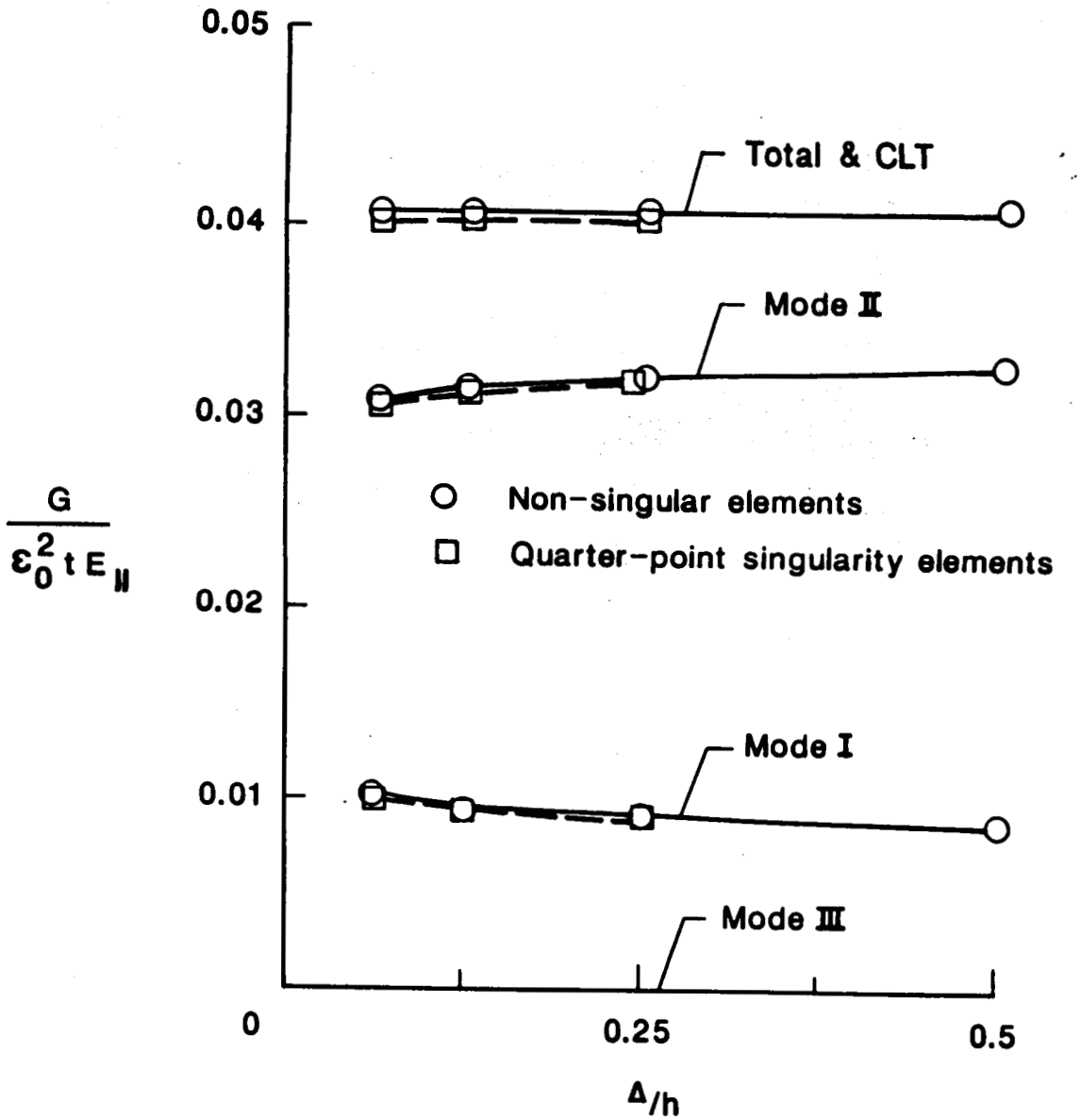

Fig.5: Comparison of strain energy release rates obtained with non-singular and quarter-point singularity elements

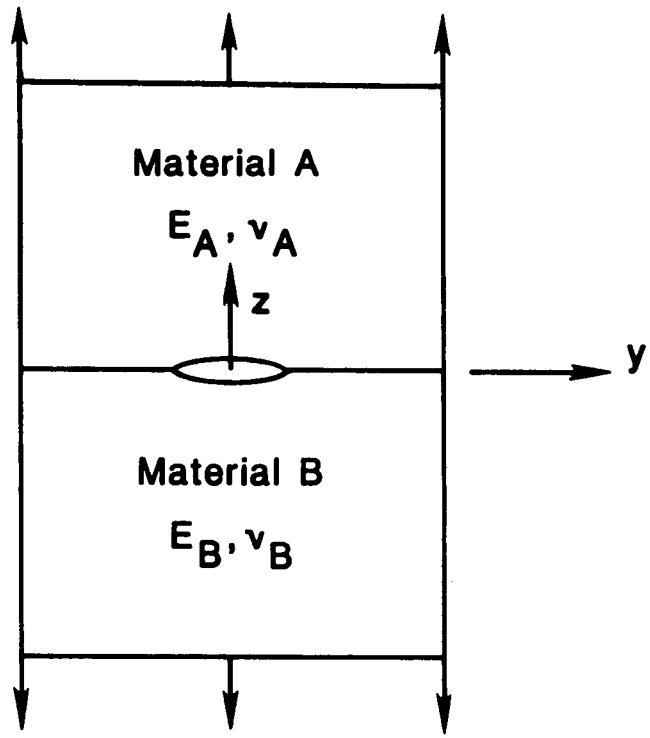

Fig.6: Bi-material plate with an interfacial crack

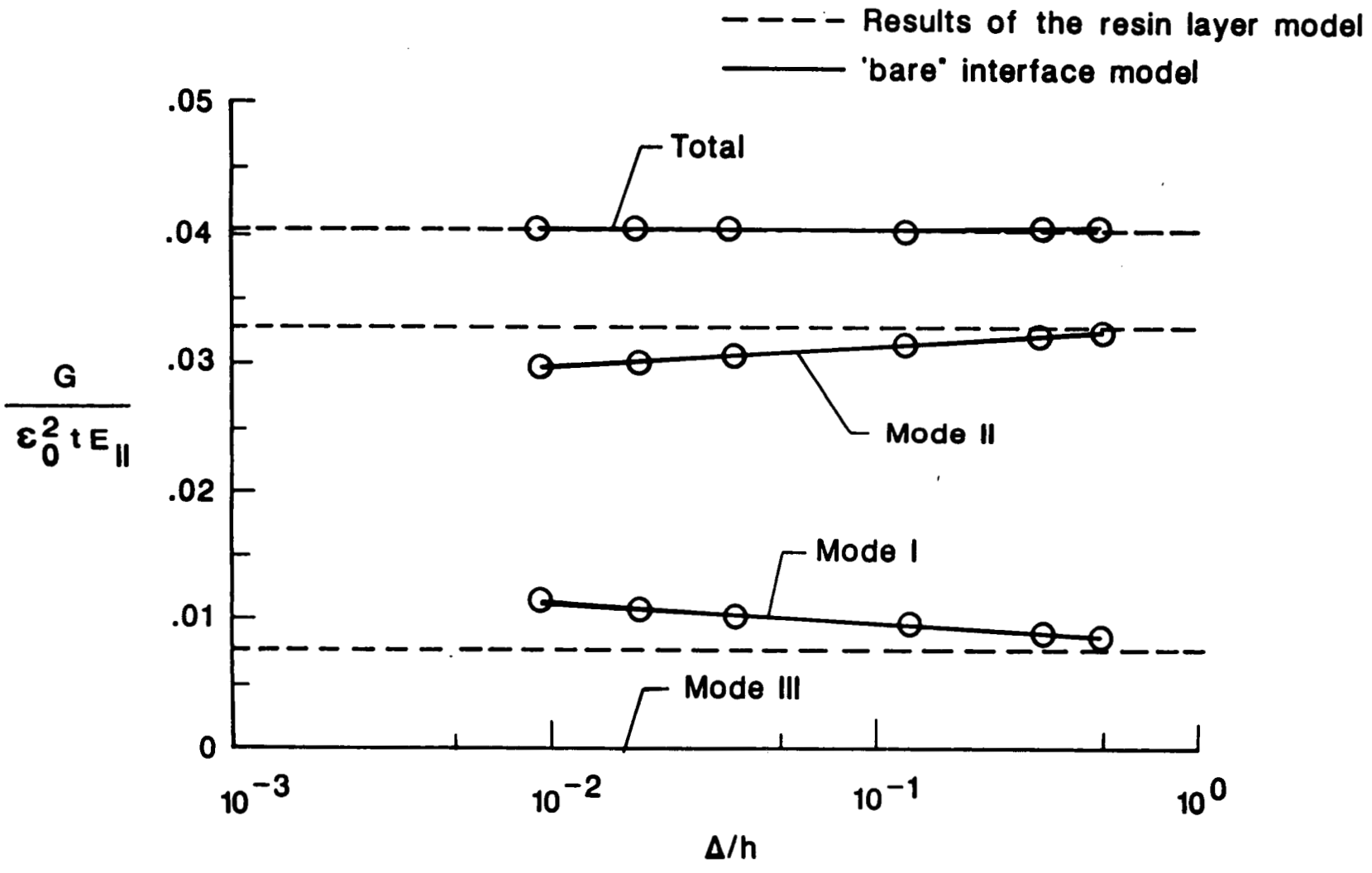

Fig.7: Comparison of strain energy release rates from the resin layer and "bare" interface models

Standard Bibliographic Page

1. Report No.	2. Government Accession No.	3. Recipient's Catalog No.
NASA TM-89135		

4. Title and Subtitle	5. Report Date
Convergence of Strain Energy Release Rate Components for Edge-Delaminated Composite Laminates	April 1987
	6. Performing Organization Code
7. Author(s)	8. Performing Organization Report No.
I. S. Raju, J. H. Crews, Jr., and M. A. Aminpour	
9. Performing Organization Name and Address	10. Work Unit No.
National Aeronautics and Space Administration Langley Research Center Hampton, VA 23665-5225	505-63-01-05
	11. Contract or Grant No.
12. Sponsoring Agency Name and Address	13. Type of Report and Period Covered
National Aeronautics and Space Administration Washington, DC 20546	Technical Memorandum
	14. Sponsoring Agency Code

15. Supplementary Notes

I. S. Raju and M. A. Aminpour, Analytical Services and Materials, Inc., Hampton, Virginia.
J. H. Crews, Jr., Langley Research Center, Hampton, Virginia.

16. Abstract

Strain energy release rates for edge-delaminated composite laminates were obtained using quasi three-dimensional finite element analysis. The problem of edge-delamination at the -35/90 interfaces of an eight-ply $[0/\pm35/90]_s$ composite laminate subjected to uniform axial strain was studied. The individual components of the strain energy release rates did not show convergence as the delamination tip elements were made smaller. In contrast, the total strain energy release rate, G, converged and remained unchanged as the delamination tip elements were made smaller and agreed with that calculated using a classical laminated plate theory. The studies of the near-field solutions for a delamination at an interface between two dissimilar isotropic or orthotropic plates showed that the imaginary part of the singularity is the cause of the nonconvergent behavior of the individual components. To evaluate the accuracy of the results, an eight-ply $[0/\pm35/r/90]_s$ laminate with the delamination modeled in a thin resin layer, that exists between the -35 and 90 plies, was analyzed. Because the delamination exists in a homogeneous isotropic material, the oscillatory component of the singularity vanishes. The strain energy release rates remained unchanged as the delamination tip elements were made smaller. Comparison of the strain energy release rates for the "bare" interface laminate, i.e., one without the resin layer, and for the laminate with the resin showed that the "bare" interface models are a very good approximation for the resin case if the delamination tip elements were one-quarter to one-half of the ply thickness.

17. Key Words (Suggested by Authors(s))	18. Distribution Statement
Strain energy release rate Delamination Composites Fracture mechanics Singularity Finite-element analysis	Unclassified - Unlimited Subject Category 39

19. Security Classif.(of this report)	20. Security Classif.(of this page)	21. No. of Pages	22. Price
Unclassified	Unclassified	40	A03

For sale by the National Technical Information Service, Springfield, Virginia 22161